

Comparative analysis in thermal behaviour of common urban building materials and vegetation and consequences for urban heat island effect

Stache, E. (Eva) ; Schilperoort, B. (Bart) ; Ottele, M. (Marc); Jonkers, H.M. (Henk)

DOI

[10.1016/j.buildenv.2021.108489](https://doi.org/10.1016/j.buildenv.2021.108489)

Publication date

2022

Document Version

Final published version

Published in

Building and Environment

Citation (APA)

Stache, E., Schilperoort, B., Ottele, M., & Jonkers, H. M. (2022). Comparative analysis in thermal behaviour of common urban building materials and vegetation and consequences for urban heat island effect. *Building and Environment*, 213, 1-10. Article 108489. <https://doi.org/10.1016/j.buildenv.2021.108489>

Important note

To cite this publication, please use the final published version (if applicable).
Please check the document version above.

Copyright

Other than for strictly personal use, it is not permitted to download, forward or distribute the text or part of it, without the consent of the author(s) and/or copyright holder(s), unless the work is under an open content license such as Creative Commons.

Takedown policy

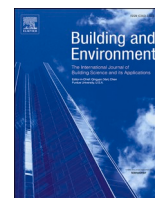
Please contact us and provide details if you believe this document breaches copyrights.
We will remove access to the work immediately and investigate your claim.

Green Open Access added to TU Delft Institutional Repository

'You share, we take care!' - Taverne project

<https://www.openaccess.nl/en/you-share-we-take-care>

Otherwise as indicated in the copyright section: the publisher is the copyright holder of this work and the author uses the Dutch legislation to make this work public.



Comparative analysis in thermal behaviour of common urban building materials and vegetation and consequences for urban heat island effect

E. (Eva) Stache^{a,*}, B. (Bart) Schilperoort^b, M. (Marc) Ottelé^a, H.M. (Henk) Jonkers^a

^a 3MD Department, Delft University of Technology (TU Delft), Faculty of Civil Engineering and Geosciences, Stevinweg 1, 2628, CN, Delft, the Netherlands

^b Department Water Management, Stevinweg 1, 2628, CN, Delft, the Netherlands

ARTICLE INFO

Keywords:

Urban heat island
Urban energy balance
Urban vegetation
Sensible heat
Latent heat
Climate resilient city

ABSTRACT

The urban heat island, is a serious threat for the urban well-being, and can be determined by the local energy balance. The surface energy balance, with respect to incoming radiative energy and subsequent partitioning into reflected energy (albedo), absorbed energy and further partitioning of latter into convective heat (Q_{Hl}), radiative heat (Q_R) and latent heat (Q_E) by using commonly applied urban materials and vegetation types, was therefore experimentally quantified in this study. In agreement with previous studies it was found that materials convert most of absorbed energy into convective heat (>92%) while vegetation channels a substantial part of absorbed radiative energy into latent heat (27–50%). It is for the first time experimentally demonstrated that significant differences in thermal behaviour between different types of urban vegetation surfaces occur. Of the investigated vegetation types ivy and moss showed respectively the highest (0.10) and lowest (0.07) albedo, but sedum and moss channelled respectively lowest (27%) and highest (50%) percentage of the absorbed radiative energy into latent heat production. Of the four investigated plant types, moss appeared most effective in preventing UHI, converting only 50% of incoming radiative energy into convective heat, while sedum was least effective converting 73% of incoming radiative energy into convective heat. These quantitative measurements show that strategic use of specific types of urban vegetation surfaces, instead of commonly applied building materials, can be an effective measure for mitigation of UHI leading to improved climate resilient cities.

1. Introduction

The urban heat island phenomenon (UHI) was first described by Luke Howard in 1818 referring to London [1]. In 1976 UHI was defined by Oke, as the warmer urban canopy layer compared with its rural neighbourhood [2]. There is agreement today that UHI has a negative effect on health, work efficiency, social life and economy and that its mitigation should therefore be an important scope for climate adaptive measures (e.g. Refs. [3,4]).

Urban morphology, building density and street configuration have a decisive influence on local urban climate, especially during heat waves [5]. Moreover, a recent study demonstrated that differences in urban morphology and type of present surface materials result in spatial differentiation of air temperature within the city space [6]. As a possible structural solution, white surfaces have been investigated with the conclusion that reflection is an efficient means for reducing absorbed solar energy. However, in streets with a cross section comparable to a canyon (where width is equal to height) or wider, the reflected

shortwave radiation will be sent to the street surface, which is usually no longer white, but mostly asphalt or concrete. This means that the local heat island will not decrease but will be increased [3].

Santamouris analysed the effect of an increased albedo of the city surface and found an average decrease of the peak ambient temperature between 0.3 and 0.9 K. In contrast, green roofs applied at the city scale produce a reduction between 0.3 and 3K [7]. Andoni argues that building skin insulation could reduce the intensity of UHI by reducing heat emissions through heavy building components [8].

In previous research it was concluded that the absence of vegetation can be linked to daily and nocturnal UHI occurrences in the built up environment [9]. An increase of hard abiotic surface areas, including facades, result in increase of UHI [10]. However, it was shown that application of large and interconnected green patches can mitigate this effect [11]. This ameliorating effect of vegetation on UHI was also found in previous studies to be the most effective and sustainable mitigation method (e.g. Refs. [12,13] and horticultural interventions were, in addition to UHI mitigation, shown to significantly improve human

* Corresponding author.

E-mail address: estache@tudelft.nl (E.(E. Stache).

well-being in the built up environment [14]. In other studies it was found that urban vegetation contributes not only to a decreasing UHI, but also to improved air quality, retention of rainwater and reduction of noise disturbances (e.g. Refs. [15–17]). Further clarification and quantification of the effect building materials have on UHI, and to what extend application of vegetation can contribute to reduce UHI, will help to improve mitigation strategies [18]. Therefore, in this research measurements were made of the energy balance of various building materials and urban vegetation in a closed, laboratory environment, with the aim of exploring the energy transfers without external influences.

1.1. Theory

Thermal behaviour of building materials in an outdoor environment is dependent on their density, heat capacity, thermal conductivity, and also on their contribution to the UHI [19]. The contribution to UHI is realized through the interaction of the surrounding air with the surface of the material. The contribution to UHI is realized through the interaction of the surrounding air with the surface of the material.

The occurrence of UHI is essentially caused by conversion of incoming solar energy into convective heat at the city surface level. Due to the dominant presence of hard surface materials in urban areas, most absorbed solar energy is transformed into convective (sensible) heat, rather than latent heat, as happens in rural areas due to the presence of vegetation [20]. The absorbed solar energy is the incoming solar radiation minus the part that is reflected by the urban surfaces. The amount of reflection is mainly determined by the surface property albedo as defined in equations (1) and (1a).

$$Q_r = r \cdot Q_{i\downarrow} \quad (1)$$

$$Q_a = (1 - r) \cdot Q_{i\downarrow} \quad (1a)$$

where $Q_{i\downarrow}$ (W/m^2) is the incoming radiative energy, r is the albedo of the material (dimensionless), Q_r (W/m^2) the reflected radiative energy, and Q_a (W/m^2) is the radiation absorbed by the surface (Incropera et al., 2017). The absorbed radiative energy is converted by the surface material into convective heat, heat storage change, longwave radiation and latent heat. The latter due to evaporation of moisture from damp or wet surfaces and evapotranspiration of present vegetation. The corresponding equation based on the first law of thermodynamics is:

$$Q_a = Q_H + Q_C + Q_R + Q_E \quad (2)$$

Where Q_H (W/m^2) is the convective heat, Q_C (W/m^2) is the change in stored heat, Q_R (W/m^2) is the net outgoing - incoming longwave radiation from the surface, and Q_E (W/m^2) is the latent heat of evapotranspiration [21].

Q_H , the convective heat transfer, is driven by the temperature gradient between the material surface and the surrounding air, and is facilitated by wind and turbulence. The higher the temperature difference, the more conversion of absorbed surface energy into convective heat will take place. In case of zero temperature difference, no conversion of absorbed energy into convective heat will take place. Production of convective heat contributes to an increased air temperature and its decrease is therefore a way to mitigate UHI [21].

Q_C , the conduction heat transfer, is driven by the temperature difference between the exterior and interior surface of the involved material. Conduction transfers the energy in form of heat through the material mass. As such, it hardly contributes to immediate warming up of the material surface. However, its stored heat will be released into the environment when the incoming radiation decreases. As a consequence, heat storage usually contributes to increase of convective heat transfer and UHI, albeit with a delay in time. In this research therefore the change in stored heat was considered to contribute to UHI in form of convective heat in accordance to the study of Hoelscher [20].

Production of thermal long wave radiation Q_R is driven by the

temperature gradient between the material surface and the sky, surrounding air, and the surfaces of nearby objects. The contribution to the heating of the surrounding air is generally negligible, and the main focus is on nearby objects receiving this radiation. As a consequence, surrounding objects may still contribute to heating up of the air (UHI) through conversion of received long wave radiation into higher surface temperature and consequently into convective heat. The amount of absorbed longwave radiation by surrounding urban objects highly depends on the local urban morphology [22]. Q_R is determined by the difference between incoming and outgoing longwave radiation.

Production of Q_E , or the latent heat of evaporation by wet and damp material surfaces and evapotranspiration by vegetation, is the part of the absorbed energy that is used for a phase change of liquid water into water vapour. Production of latent heat is taking place, as long as sufficient water supply is available for evaporation or evapotranspiration by material surfaces and vegetation respectively. The water vapour will be transported outside of the urban system boundary, to higher atmospheric layers, thus not contributing to UHI [23].

1.2. Aim of the research

Research concerning the energy balance of the urban space has increased in the last decades due to the recognition of the role urban building materials and the urban morphology play in it [24], involving both outdoors and laboratory based investigations (e.g. Refs. [19,25]). Although these studies provided a base for better understanding of the UHI phenomenon and the mitigation potential by urban vegetation, direct experimental quantitative comparison of energy conversion of specific urban surface materials and common types of urban vegetation is still missing.

Insight into the extend urban materials and vegetation types reflect incoming solar radiation (albedo) and convert absorbed energy into Q_H , Q_R , and Q_E and thus potentially contribute to or mitigate UHI is important in order to improve knowledge and essential for designing climate resilient urban environments. The main aim of this study therefore was to experimentally quantify and compare albedo, along with the ratio between Q_H and Q_E produced by some typical urban surface materials and vegetation. Key parameters to be quantified were the albedo, amount of thermal radiation, amount of sensible heat produced by specific urban materials, and latent heat produced by vegetation as these influence to a major extend UHI in cities.

2. Materials and experimental setup

2.1. Materials

Two different series of specimens were investigated in this study, one comprising different urban building materials and one consisting of living vegetation types commonly used to cover horizontal (or vertical) urban surfaces. According to the literature reviewed (see Table 1 and 2), the materials studied are among the most commonly used in Dutch architectural practice. In the urban space investigated in the

Table 1

Types and typical application areas of investigated building materials and documentation reference in which more detailed information on these materials can be found.

Type	Field of use	Reference
Brick (red)	Façade, street	[19]
Concrete	Building, façade, street	[19]
Pinewood	Building, façade, roof	[26]
wood WRC	Building, façade, roof	[26]
HPL (white)	Façade	https://www.trespa.com/
HPL (black)	Façade	https://www.trespa.com/
Bitumen	Roof, street	https://derbigum.be
Plastic plant		

Table 2

Species and typical application areas of investigated types of urban vegetation and reference to publications concerning urban studies in which these species were featured.

Latin name	Common name	Field of application	Reference
<i>Scleropodium purum</i>	Moss	Roof	[27]
<i>Poa pratensis</i>	Grass	Gardens, parks, street sides	[11]
<i>Hedera helix</i>	Ivy	Façade, roof	[17]
<i>Sedum album</i>	Sedum	Roof	[28]

Netherlands, the materials studied make up most of the surfaces. The influence of their thermal behaviour could be seen as of significant importance for outdoor spaces of the Dutch cities. Similar investigations should be conducted in other cities with different, locally typical, building materials and vegetation types in order to determine the local effect on the UHI.

Building materials like bricks, concrete tiles, pinewood, western red cedar wood (WRC), bitumen, and white- and black coloured HPL, i.e. high pressure synthetic polymer laminate (wood fibre/phenolic resin composite) are commonly used urban building materials and typically applied as cladding (surface finishing) (Table 1).

Investigated vegetation types comprises moss, grass, ivy and sedum as these are also commonly found or applied as surface materials in urban environments (Table 2). A plastic plant (ivy lookalike) was added to the list of building materials in order to compare its impact and (energy) behaviour to that of living plants.

Although many species of vegetation are found in urban areas [27], only a few species that are commonly applied on streets or building facades and roofs [17] were investigated in this study to clarify whether substantial differences in energy behaviour, with respect to albedo, and conversion of net radiative energy into Q_H and Q_E between these types

occur.

It is important to note that the production of Q_H and Q_E is very dependent on variables such as the wind speed, soil moisture, and plant physiology (e.g. heat stress). These effects were not taken into account in this study, and as such only an indication of the ratio Q_H/Q_E can be provided. For outside conditions the ratio Q_H/Q_E would have to be determined using other methods, such as the Penman-Monteith equation for potential evaporation (<http://www.fao.org/3/x0490e/x0490e06.htm>).

The living plants were investigated in association with the soil or substrate in which they rooted. Although the plant leaf density was at higher than 3 in most cases to completely cover of the underlying substrate (see Fig. 1), some effect of substrate on conversion ratio of absorbed radiative energy to Q_H , Q_R and Q_E cannot be excluded. Typically Q_E , representing transpiration of vegetation, may therefore have been overestimated specifically for grass LAI 4.70 while in literature 1.25–1 [29], as moisture evaporation from the underlying substrate may have contributed to Q_E . In case of Ivy the substrate in which it rooted could be left outside and isolated from the measuring area, ensuring that the determined Q_E was solely due to the plant biomass. See Fig. 1 for pictures of the materials and vegetation types investigated in this study. Investigated surface area was 0.6×0.6 m equalling 0.36 m². In addition, a similar surface of water was investigated to be compared to the evaporation trends of the vegetation samples.

2.2. Experimental setup

The laboratory based setup was designed to simulate solar radiative energy burden on common urban materials and often used vegetation on buildings in a horizontal setup, during heat wave periods during which UHI typically occurs. The research focused on the influence of

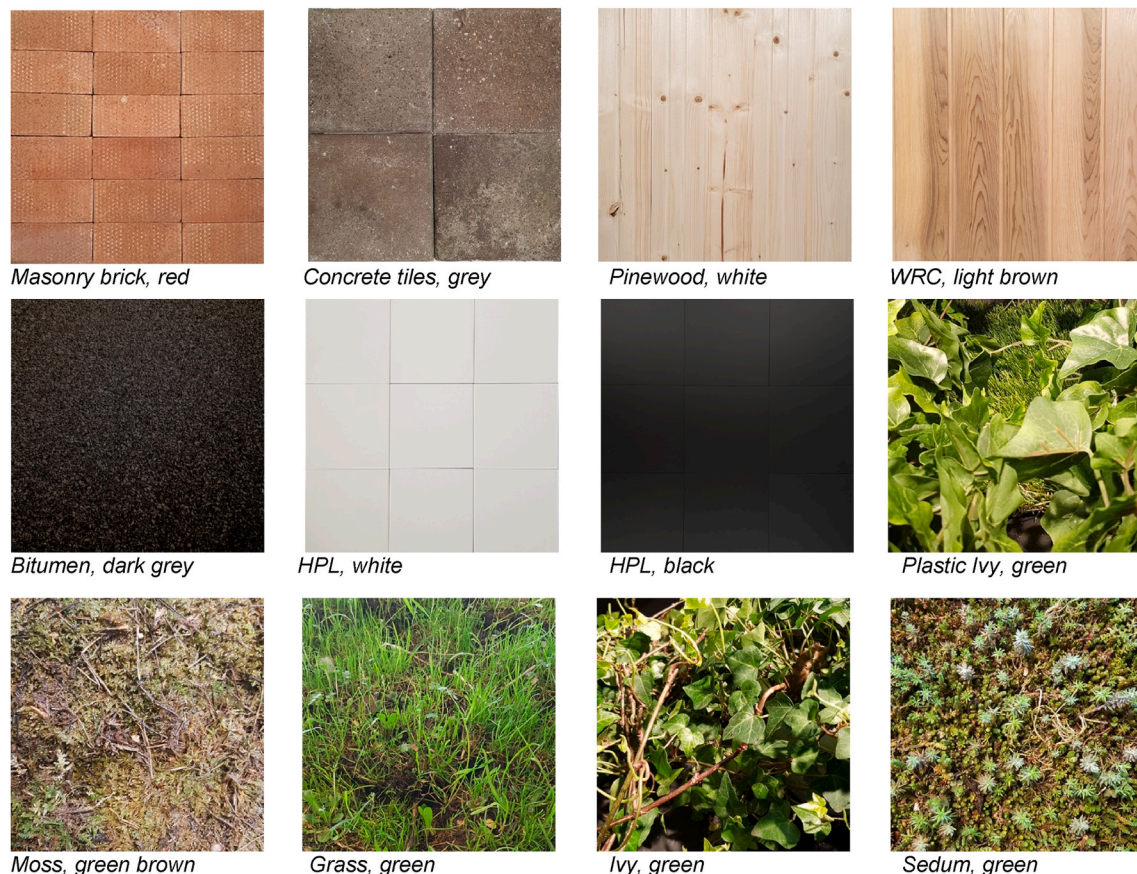


Fig. 1. Images of the investigated materials and vegetation.

evaporation on the energy balance of the outdoor space. In this study, no research has been done into the influence of the evaporation on the inside of the wall, since this would concern the interior space.

The investigated objects were exposed for 4-hour periods to about 1000 Watt of incoming artificial illumination (spectrum 90–100 CRI, Coloring Rendering Index) provided by two 500 Watt compact theatre spot lights. The light period was followed by 4 h hours of darkness (cooling). This light/dark sequence period was adopted from a previous conducted by Ref. [19]; where a 4 h hour light and 4 h hour dark period was shown sufficient for reaching temperature steady state conditions [19]. Illumination intensity of around 1000W on a surface area of 0.36 m² was chosen as this appears a typical light exposure in urban settings during heat wave periods according to the Dutch meteorological institute [30]. The actual incoming radiation on the surface of test specimen placed in the experimental setup was quantified by a CNR4 Net Radiometer (Kipp & Zonen BV, Netherlands), consisting of a pyranometer pair, one facing upward, the other facing downward, and a pyrgeometer pair in similar configuration. The upward and downward facing pyranometers and pyrgeometers measured the incoming and reflected shortwave- and longwave radiation respectively. The radiometer was connected to a Campbell CR6 data logger with a sampling rate of

2 min minutes (Kipp & Zonen BV, Netherlands). The radiometer was calibrated relative to a reference radiometer according to the suppliers' manual. Surface temperature dynamics of investigated materials and vegetation was measured by two thermocouples type K connected to a Testo 176 T4 datalogger with a sampling rate of 2 min minutes (<https://www.testo.com/nl-NL/testo-176-t4/p/0572-1764>). Air temperature dynamics at a distance of 0.1 m above the samples were measured and recorded using a Testo 174 H - WiFi data logger with a sampling rate of 2 min minutes and with integrated temperature sensor (<https://www.testo.com/nl-NL/search/?text=testo+0572+0566>). See Fig. 2 for a schematic drawing, and Fig. 3 for some pictures of the laboratory based measuring setup.

The light spectrum included the total visible wavelengths between 380 nm and 750 nm. The room temperature during the measurements was 20 °C. The air around the specimen was stagnant, except the air velocity induced by the temperature differences. The speed of this air velocity was 0,3 m/s in vertical direction.

The material or vegetation samples were lined up horizontally, referring to all horizontal surfaces in the urban outdoor space, such as flat roofs and streets or squares. The most relevant urban surfaces have either a horizontal or a vertical orientation. Horizontal and vertical

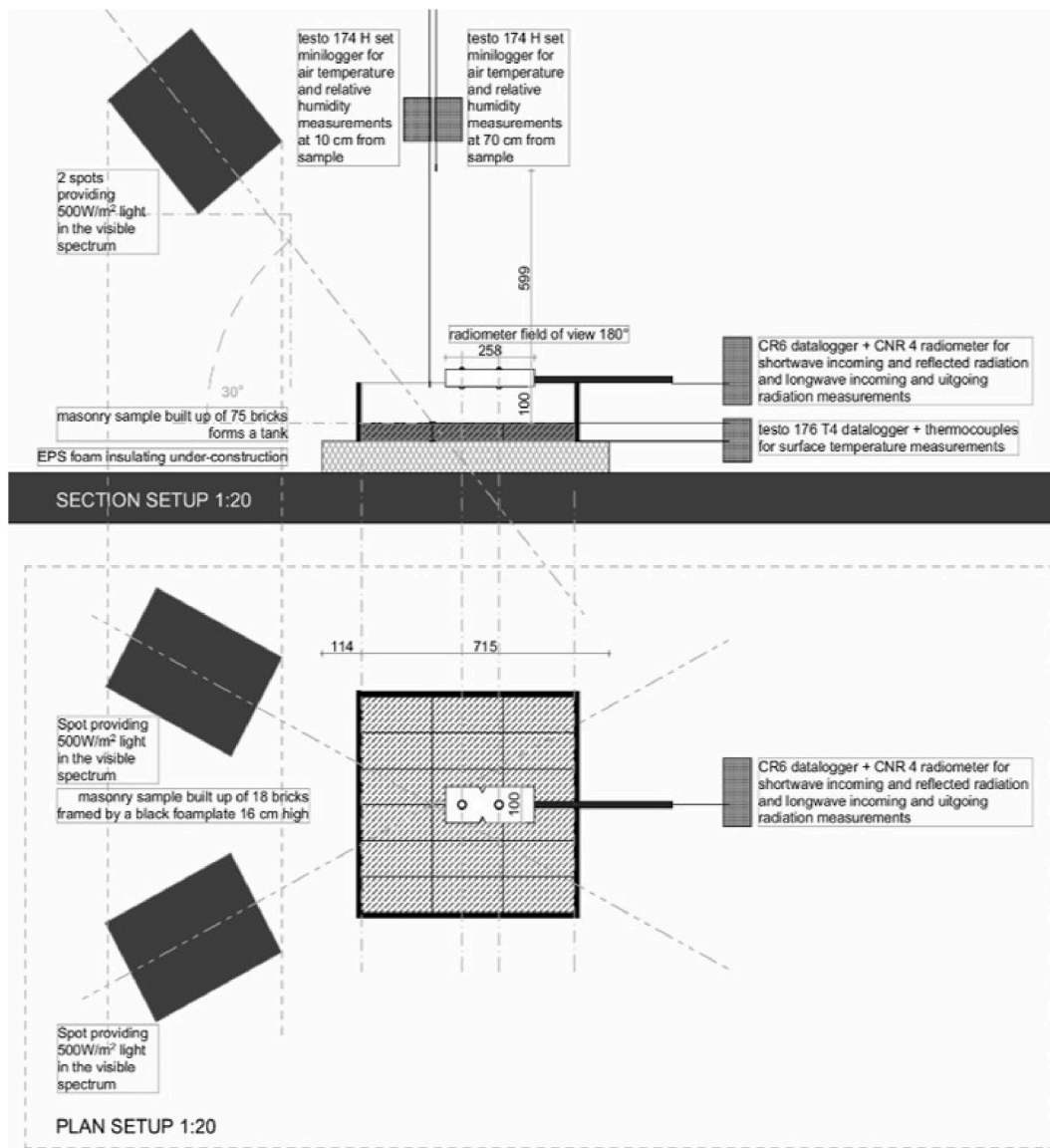


Fig. 2. Schematic drawing of the experimental setup.

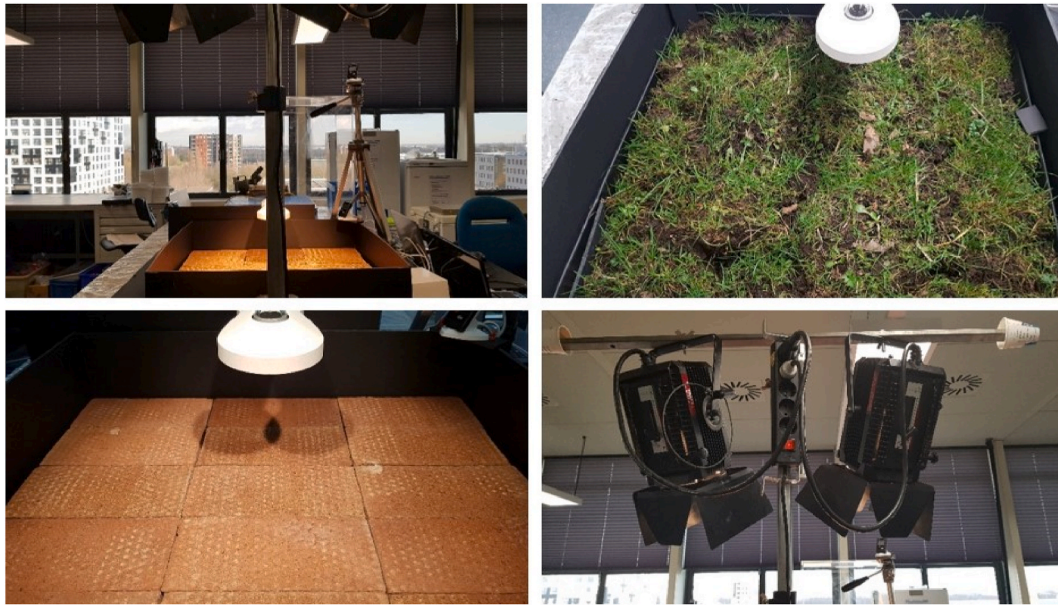


Fig. 3. Pictures of the experimental setup showing an overview of the setup (top left picture), bricks- and grass samples (bottom left and top right pictures respectively) and the theatre spot light source (bottom right picture).

surfaces receive solar radiation at different angles and therefore the calculation methods for convection are also different. The research question, however, was not to demonstrate the difference between the horizontal and vertical measurements.

The samples were placed on a styrofoam base layer with dimensions of $1 \times 1 \times 0.09$ m. This insulation material has an R_d value of $0.8 \text{ m}^2\text{K}/\text{W}$ and was assumed to form an effective insulation layer (with respect to the illumination sequence) between the sample and the table on which the setup was mounted. The surface area of samples was set at 0.6×0.6 m. An edge of 0.16 m height and 0,04 thickness of black styrofoam plates was built around the sample in order to ensure minimal lateral light disturbances from the laboratory environment during radiometer measurements. The radiometer was placed at a height of 0.16 m from the sample surface. The light sources, composed by the two theatre spots, were placed next to each other and set at an angle of 30° measured from the vertical direction (90°). This angle falls within the angles made by the sun during the summer month (June, July and August) between 10 a.m. and 2 p.m. in the Netherlands, where the location of the test was ($50.17^\circ - -50.17^\circ$). The angle of 30° was chosen to minimize formation of shadow from the radiometer on the sample surface. (as it happens in case of an angle of 90°) The sensors for surface temperature measurements were placed at the surface and the backside of the samples. An exception to the standard sample dimensions was the ivy as it had a different shape due to the long leave stalks. This allowed placement of the plant pot outside the measuring area but the plant leaves inside of the measuring area.

3. Methodology

Measurements were done according to the protocol of 4h light and 4h cooling described by Wonorahardjo [19]. Samples were before the actual start of measurements left to adapt to the laboratory conditions for 16 h hours. Each sample was placed on the insulating Styrofoam base-layer and exposed to illumination during a 4 h hours-period in which a temperature steady state situation was reached, followed by a 4 h hours cooling period to allow cooling down of the samples. Vegetation samples were weighed in gram before and after the light/dark measurement period to establish the amount of water loss due to evapotranspiration. Measurements of temperature dynamics of materials and vegetation subjected to light/dark periods were used as input

for estimation of Q_H , Q_R and Q_E values. In this study it was assumed that results obtained under laboratory conditions are representative for the thermal behaviour of the materials exposed to outdoors solar radiation and that the investigated building materials were homogeneous and dry and therefore not producing any latent heat.

3.1. Determination of material properties

Density of materials was determined by volumetric dimensions and weight. The biomass (density) of vegetation was estimated through leaf area index (LAI) analysis. The LAI of moss was approximated by visual estimation of the leaves coverage per moss layer multiplied by the number of present layers of leaves. The LAI of grass, sedum and Ivy was determined by counting the number of leaves in a surface area of 10×10 cm assuming this to be representative for the area under investigation. The average leaf area was determined by making a scan of the largest and smallest leaf and by determining their surface area.

3.2. Procedures for determination of parameters involved in energy flow and conversion

For quantification of albedo, Q_a (energy absorbed by materials), Q_H (convective heat), Q_R (outgoing longwave radiation) and Q_E (latent heat production) the following measurements were done:

- Quantification of the incoming and outgoing short- and longwave radiation related energy at the material surface through radiometric measurements
- Quantification of the albedo of the materials by dividing outgoing shortwave-by incoming shortwave radiation measured by the respectively downward- and upward facing pyranometers
- Quantification of Q_a by subtracting outgoing shortwave radiation related energy from incoming shortwave radiation related energy as determined by the pyranometer measurements
- Quantification of Q_R by subtracting outgoing longwave radiation from incoming longwave radiation as measured by the respective downward- and upward facing pyrgeometers
- Quantification of material and vegetation surface temperature (T_s) measured by the Testo 176H

From these measurements values albedo, Q_w , Q_H , Q_R and Q_E could be calculated as described further down below. An overview of the way parameter values were either measured or calculated is shown in Table 3.

Quantification of Q_H (convective heat in W/m^2) for materials was done according to equation (2) in which Q_H equals the amount of absorbed energy (Q_a) minus the emitted amount of long wave radiative energy (Q_R) as Q_C (conductive heat) is assumed to be converted to Q_H within the measurement period and Q_E (latent heat) is assumed to be negligible for dry materials.

$$Q_H = Q_a - Q_R \quad (2)$$

The convective heat produced by vegetation (Q_{Hv} , W/m^2) was calculated according to equation (3) in which Q_{Hv} equals the amount of absorbed energy (Q_{av}) minus the emitted amount of long wave radiative energy (Q_{Rv}) and minus the calculated latent heat (Q_E)

$$Q_{Hv} = Q_{av} - Q_{Rv} - Q_E \quad (3)$$

Values for Q_E produced by vegetation were calculated by measuring the weight difference of the vegetation samples between the start and the end of the light/dark period multiplied by the value of latent heat of water evaporation ($h_{fg} = 2441,7$ kJ/kg at 295K according to Incropera, 2017) (equation (4)).

$$Q_E = H_{fg} \cdot \Delta_{water} \quad (4)$$

Where H_{fg} is the latent heat of evaporation (kJ/kg) and Δ_{water} is the weight difference at the beginning and the end of the measurement period (kg/s).

4. Results

4.1. Comparison of materials and vegetation albedo

Albedo of materials and vegetation types was determined by measuring incoming shortwave radiation and reflected shortwave radiation and calculating the ratio between them. Results are shown in Table 4.

The determined albedos for the specific materials and vegetation types largely agree with within the range of albedos for materials as found in literature. Interesting to note is that the albedos of the vegetation types investigated in this study are relatively low in comparison to

Table 3

Overview of measured and calculated parameters considered in this study.

Parameter	Symbol	Measured/calculated	Device
Albedo	r	Outgoing shortwave radiation/incoming shortwave radiation	pyranometer
Incoming shortwave radiation	S_{\downarrow}	Measured	pyranometer
Outgoing shortwave radiation	S_{\uparrow}	Measured	pyranometer
Incoming longwave radiation	L_{\downarrow}	Measured	pyrgeometer
Outgoing longwave radiation	L_{\uparrow}	Measured	pyrgeometer
Emissivity (broad spectrum)			
Absorbed energy by the surface	Q_a	Incoming shortwave radiation - Outgoing shortwave radiation	
Convective heat	Q_H	Calculated, see text	
Thermal radiation from the surface	Q_R	Outgoing longwave radiation - incoming longwave radiation	
Latent heat	Q_E	Calculated, see text	
Surface temperature	T_s	Measured	Testo 176H
Leaf Area Index vegetation	LAI	Measured and calculated	

Table 4

Ratio between reflected (SW_{lower}) and incoming (SW_{upper}) shortwave radiation (albedo) of materials and vegetation as determined in this study and reported values in literature.

Material/vegetation	Determined albedo	As found in literature albedo	Literature reference
Brick	0.26	0.20–0.40 0.3	[21] [31]
Concrete	0.13	0.10–0.35 0.4	[21] https://gccassociation.org/sustainability-benefits-of-concrete/albedo/
Bitumen	0.02	0.05–0.20 0.32	[21] [32]
Pinewood	0.35		
wood WRC	0.31		
HPL white	0.35	0.20–0.40	[21]
HPL black	0.03	0.02–0.15	
Plastic plant	0.06	0.16	[33]
Moss	0.07	0.11	[34]
Grass + soil	0.09	0.16–0.26 0.05–0.40	[21] [35]
Ivy	0.10	0.09	[21]
Sedum	0.09		
Water	0.14	0.03–0.10 0.06	[21] https://nsidc.org/cryosphere/seaice/processes/albedo.html

the materials. Albedo of vegetation types range between 0.07 and 0.10 which is higher than typical dark material as bitumen (0.02) and black HPL (0.03) but substantially lower than common surface materials like concrete (0.13), brick (0.26), timber (0.31–0.35) and white HPL (0.35). The albedo of the tested green plastic ivy lookalike (0.06) was found to be somewhat lower than that of its living analogue (0.10). It can be concluded from the obtained data that vegetation on average absorbs more incoming radiation in comparison to common surface building materials.

4.2. LAI and evapotranspiration of vegetation

The leaf area index (LAI) of the investigated vegetation types was determined in order to quantify the actual vegetation surface area per area covered by vegetation. Moreover, the actual surface area is the area that affects Q_E (production of latent heat) through the process of evapotranspiration. Table 5 shows the LAI values of the vegetation types as determined in this study in comparison to typical values of previously published studies. It shows that the obtained LAI values determined in this study were largely congruent with average LAI values documented in literature for ivy and sedum, and were respectively lower and higher for moss and grass. The weight loss of vegetation during an 4h light and 4h cooling measuring period was also determined and this was assumed to be due to the process of evapotranspiration. Weight loss during the 8 h hours measuring period are also shown in Table 5 for the vegetation types investigated in this study.

The ratio of weight loss and LAI show that evapotranspiration over the measured 8-hour period per leaf area is highest for grass (0.263) and lowest for sedum (0.109). This ratio is an expression of the evapotranspiration performance which is determined by the stomatal conductance's influence specific for the different vegetation types, the LAI, the energy supply, vapour pressure gradient and wind [21]. However, taking the specific vegetation leaf density into account, the weight loss measurements show that the rate of evapotranspiration per vegetation surface area per hour of light period is highest for moss (0.33 kg . $m^{-2} h^{-1}$ light period), followed by grass (0.30 kg . $m^{-2} h^{-1}$ light period), Ivy (0.22 kg . $m^{-2} h^{-1}$ light period) and sedum (0.19 kg . $m^{-2} h^{-1}$ light period).

Table 5

The weight loss, the LAI of vegetation types determined in this study in comparison to values reported in literature and the ratio of weight loss and LAI.

	weight loss during 4h licht + 4h dark measuring period	LAI calculated	Ratio weight loss(kgm ⁻²)/LAI (m ² m ⁻²)	LAI according to literature	literature
Moss	Kg/0.36m ² 0.48	m ² m ⁻² 8.80	0.153	m ² m ⁻² 15.7 ± 4	[36]
Grass	0.43	4.54	0.264	1.6–4.9	[37]
Ivy	0.32	3.70	0.239	1.25–1.00	[29]
Sedum	0.27	6.80	0.109	0.61–5.7	[38]
				3.50	[39]
				2.6–7.7	[40]
				5.94	[41]
				4.5	https://www.nparks.gov.sg/florafaunaweb/flora/April 2, 2449

4.3. Determination of Q_H, Q_R and Q_E of materials and vegetation

In order to clarify whether vegetation can play a significant role in mitigation of the UHI effect, the partitioning of absorbed radiative energy over Q_H (convective heat), Q_R (outgoing longwave radiation) and Q_E (latent heat production) for the various material and vegetation types was determined. An increase in temperature of the surface of materials and vegetation was observed during the 4 h hours illumination period and subsequent cooling down during the sequential 4 h hours dark period. An example of the observed surface temperature dynamics during an 8 h hours light/dark measuring period for one material (bitumen) and one vegetation (moss) type is shown in Fig. 4.

A clear difference that can be observed between the two materials is that the surface temperature of the bitumen increases faster and reaches a substantially higher value (58.8 °C) in comparison to the moss (maximum 37.3 °C). Interesting to note is that the time required for reaching a steady state in temperature, both after switching the light on and off, varied per material (see Table 6).

The determined amount of Q_a expressed as percentage of total incoming radiative energy, and subsequent partitioning of Q_a in Q_H, Q_R and Q_E expressed as percentage of Q_a as well as percentage of total incoming radiative energy that is converted to Q_H as determined in this study for materials and vegetation types is listed in Table 6.

Apparent from these data is that building materials (including the plastic plant) almost completely (>92%) convert absorbed radiative energy into Q_H (convective heat) while this is substantially less for vegetation (51–73%) which channel the remaining energy mostly into

Table 6

The absorbed amount of energy Q_a as percentage of S_↓ and subsequent partitioning in Q_H, Q_R and Q_E (as percentage of Q_a) and percentage of total incoming radiative energy converted to Q_H and time required to reach steady state in temperature after switching the light on and off for materials and vegetation types as determined in this study. TSS-DL is the time required to reach temperature steady state from dark to light period and TSS-LD is the time required to reach temperature steady state from light to dark.

name	Q _a of S _↓	Q _H of Q _a	Q _R of Q _a	Q _E of Q _a	Q _H of S _↓	TSS-DL	TSS-LD
	%	%	%	%	%	min	min
Masonry	74	96	4	–	71	226	196
Concrete	87	95	5	–	83	240	210
Bitumen	98	93	7	–	91	44	70
Pinewood	65	99	1	–	64	100	98
WRC	69	98	2	–	68	156	154
HPL white	65	98	2	–	63	72	126
HPL black	97	93	7	–	90	64	90
plastic plant	94	97	3	–	91	88	84
Moss	93	51	–1	50	47	58	112
Grass	91	60	–2	42	54	212	206
Ivy	90	66	1	34	59	30	110
Sedum	91	73	0	27	67	128	84
Water	86	61	0	40	52	110	144

Q_E latent heat (50-27%). However, considering that albedo plays an important role in reflecting incoming radiation, it is important to determine which part of the total incoming energy is actually converted

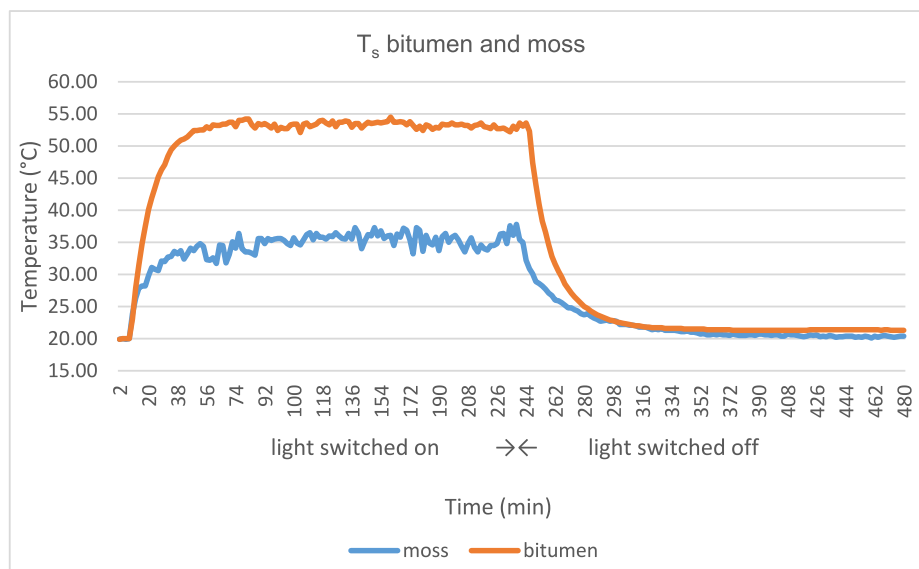


Fig. 4. Typical dynamics of the surface temperature of bitumen (blue line) and moss (orange line) during a sequential 4 h hours light and 4 h hours dark period as determined in this study. (For interpretation of the references to colour in this figure legend, the reader is referred to the Web version of this article.)

into Q_H as this contributes to a major extend to heating up of the air above the material or vegetation surface and therefore to the UHI effect. This comparative study shows indeed that albedo plays an important role as the difference between materials and vegetation in percentage of incoming energy that is converted to Q_H becomes smaller (63–91% for materials and 47–67% for vegetation). Interesting is furthermore that values between vegetation types differ substantially. While conversion of total incoming energy to Q_H is relatively high for sedum (67%) it is low for moss, grass and ivy (47%, 54% and 59% respectively).

5. Discussion

The main aim of this study was to investigate the thermal behaviour experimentally in order to quantify and compare the albedo, emissivity, and proportion of Q_H , Q_R and Q_E produced by some typical urban surface materials and vegetation. The quantified key parameters were the total incoming radiation, reflected shortwave radiation (albedo), amount of convectional (sensible) heat produced by the specific urban materials, outgoing longwave radiation and latent heat produced by vegetation as these determine to a major extend UHI in cities. The executed measurements show that a period of 4 h hours of light and 4 h hours of darkness provides sufficient scope for reaching a steady state situation and therefore it was not necessary to measure over a longer period.

The results show that the absorbed amount of radiative energy, particularly determined by the material and vegetation albedo, is not distinctive for materials or vegetation but rather type specific. E.g. green plastic and living ivy and other types of investigated vegetation show comparable albedo (0.06–0.10) while that of white HPL and pinewood are higher (0.35) and of black HPL (0.03) and bitumen (0.02) substantially lower. The lower the albedo the higher the amount of absorbed energy, and this was specifically high for the investigated low albedo building materials bitumen (98%), black HPL (97%) but also for moss (93%). However, when considering UHI, besides albedo, the capacity of surfaces to convert absorbed energy into latent heat instead of convectional heat is crucial. Table 6 shows the combined effect of albedo and latent heat production capacity of investigated materials and vegetation, as it shows the percentage of incoming radiative energy that is actually converted to convectional heat. It shows that of all investigated materials it is only the high albedo materials white HPL and timber (pinewood and WRC) that produce comparable convective heat (63–68% of incoming energy) with the four types of vegetation investigated (47–67%).

As already known from literature (e.g. Refs. [21,25]), the measurements done in this study show that next to albedo, it is particularly the capacity of evaporation and evapotranspiration that determines the actual conversion of incoming energy into convective (sensible) heat. The ratio of weight loss and LAI showed that moss, grass and ivy show the highest rate of evapotranspiration in $\text{kg water}\cdot\text{m}^{-2}$ surface covered $\cdot\text{h}^{-1}$ (0.33, 0.30 and 0.23), while sedum show the lowest (0.19) when illuminated with about $4000 \text{ W}\cdot\text{m}^{-2}$. These results offer important information for the choice of vegetation in the design process of low UHI cities.

Although the leaf area index (LAI) of moss was found to be almost twice as high as that of grass (8.80 versus $4.54 \text{ m}^2\cdot\text{m}^{-2}$), the rate of evapotranspiration per actual surface area covered appeared almost similar (0.33 versus $0.30 \text{ kg}\cdot\text{m}^{-2}\cdot\text{h}^{-1}$), resulting in a lower specific evapotranspiration versus LAI of moss in comparison to grass (0.152 versus $0.263 \text{ kg}\cdot\text{m}^{-2}$). Also, sedum shows a relatively high LAI ($6.80 \text{ m}^2\cdot\text{m}^{-2}$), while its specific evapotranspiration appears to be low ($0.110 \text{ kg}\cdot\text{m}^{-2}$). These data show that the LAI value is of limited use when choosing vegetation for optimal mitigation of UHI. These results further underline the importance of plant type choices, with regard to stomatal characteristics (determining transpiration rates) and the actual availability of sufficient water required to support maximal evapotranspiration rates.

Temperature gradient analyses of plant and material surface and air

temperature, show that during illumination vegetation generally develops a smaller gradient in comparison to building materials (e.g. see Fig. 5). This results in lower Q_H production for vegetation. To maintain a smaller temperature gradient and consequently a low Q_H but high Q_E production sufficient water supply is essential.

The temperature difference between air and material surface for moss was found to become negative quickly after switching of illumination. This means that the temperature of the moss became actually lower than that of the surrounding air. This phenomenon can be explained by the continued production of latent heat (due to evapotranspiration) in the dark period [25].

As a consequence of latent heat production by plants (in case of sufficient water supply) a smaller part of the absorbed radiative energy is converted to sensible heat. This results, as Fig. 5 illustrates, in substantially lower surface temperatures in comparison to (dry) building materials. This likely means that the lower surface temperature of vegetation is also more effective in absorbing long wave radiative heat (Q_R) typically produced by low albedo building materials. Specifically in street canyons this can further help to mitigate UHI as here produced Q_R is often absorbed by opposite walls and after all converted to Q_H by low albedo building materials what further contributes to UHI.

Although the amount of absorbed radiation by plants was high, their Q_H production was significantly lower than by other materials (66 by ivy, 93% by black HPL), showing differences between 20% and 40%. The water surface produced a comparable amount of Q_H , converting 60,68% of the absorbed energy into sensible one. The highest amount was produced by sedum (73%) and the lowest by moss (51%). Important to note that sedum can use CAM (Crassulacean acid metabolism) photosynthesis; this means that the stomata are closed during the day and only open at night. During the day there will be hardly any evaporation. The plants regulate this on the basis of temperature/dryness test pressure [42]. Switching is also not instantaneous, and can take up to a week [43].

An interesting question is to what extend vegetation is effective in lowering UHI in comparison to a water body. The latent heat (Q_E) production by water amounted to 40% of the absorbed radiative energy (Q_a), while convective heat production was 52% of total incoming radiative energy. Q_E production from absorbed energy was therefore found to be higher than that of ivy and sedum (34 and 27% respectively), but lower than that of moss and grass (50 and 42% respectively). Convective heat production by water from total incoming energy was found to be 52% and this value was lower than that of sedum (67%), ivy (59%) and grass (54%), but higher than that of moss (47%). Apparently moss does thus perform better than a water body in terms of mitigation potential of UHI. This could be due to the greater transpiration surface of the moss compared to the evaporation surface of water.

Overall, in relation to UHI mitigation potential, vegetation performed better than building materials. This is most apparent when comparing the proportion of Q_H produced from the total incoming radiative energy. Some materials, typically characterized by a relatively high albedo, like pinewood and white HPL, produced relatively low Q_H values (64 and 63% respectively), which are lower than the worst performing plant (sedum: 67%), but higher than the other investigated plants (59, 54 and 47% for ivy, grass and moss respectively). All other building materials, including the plastic ivy lookalike performed worse (ranging from 68% for WRC to 91% for both bitumen and plastic ivy). These observations once more clarify that strategic choice of type of building material, in combination with application of vegetation, can substantially lower the risk of pronounced UHI effect in cities, particularly during heat wave periods.

This result confirms previous results that plants in all cases contribute less to the forming of UHI than traditional building materials, assumed that sufficient water supply is available (e.g. Refs. [18,21,25]). However, it also concludes that there is a production of sensible heat by plants as well, even as the limited laboratorial setting may have increased this effect. The design of vegetation in urban settings needs

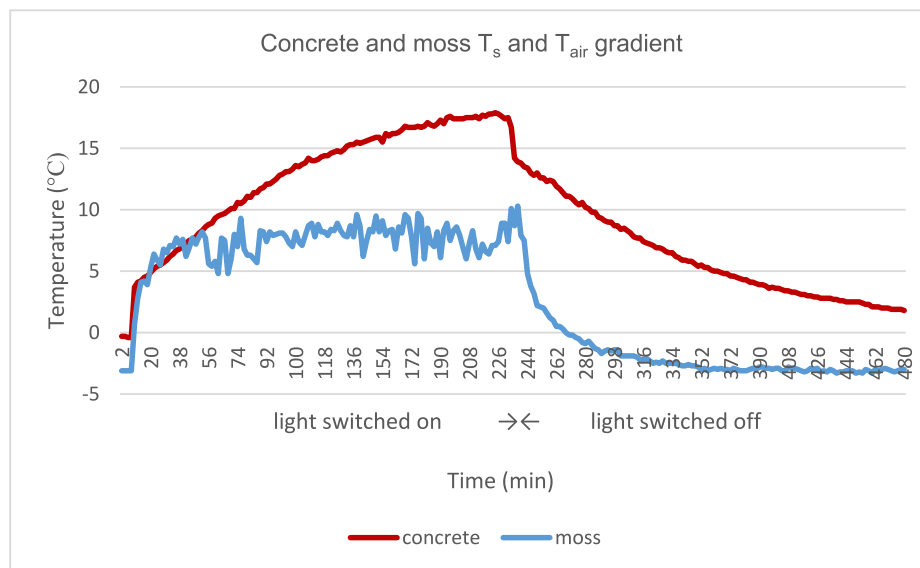


Fig. 5. Typical dynamics of the difference between surface and air temperature of concrete (blue line) and moss (orange line) during a sequential 4 h hours light and 4 h hours dark period as determined in this study. The difference in temperature for concrete steadily increases over time during the illumination period and steadily decreases during the dark period while for moss it reaches a steady state situation relatively fast (within half an hour after switching the light either on or off). (For interpretation of the references to colour in this figure legend, the reader is referred to the Web version of this article.)

therefore special attention, in order to avoid high Q_H production. Sufficient water supply is necessary to ensure a high latent heat production and a specific plant selection is needed.

6. Conclusions

In this study, the surface temperature, the albedo and the thermal radiation were determined by measurements. The distribution of the absorbed energy by the different materials and vegetation in Q_H , Q_R and Q_E were calculated based on the measurements. The lower surface temperatures developed by the vegetation (e.g. 37.3 °C compared to 58.8 °C for bitumen) results in lower temperature gradients between the surface and the surrounding air. In addition to transpiration, the lower gradient also contributes to a lower air temperature produced around vegetation, compared to the air temperature produced around common building materials.

In this study the differences between the partitioning of Q_H , Q_R and Q_E for typical building materials and vegetation types have been measured. While traditional dry urban building materials transfer most of the absorbed energy into sensible heat (between 92% and 99%) and thermal longwave radiation (between 1% and 7%), vegetation transfers a substantial amount to latent heat (between 27% and 50%). While the relatively high albedo of some building materials mitigates their UHI potential, it is vegetation that shows overall the best performance in UHI mitigation potential, as the total sensible heat (Q_H) production from total incoming radiative energy is substantially lower (from 47 to 67%) than that of the investigated building materials (63–91%).

It should be realized however, that an important requirement for plants to produce substantial amounts of latent heat is a continuous and sufficient water supply. Water supply systems must thus be integrated in green designs of cities to ensure effective UHI mitigation, particularly during prolonged heat wave periods.

Declaration of competing interest

The authors declare that they have no known competing financial interests or personal relationships that could have appeared to influence the work reported in this paper.

References

- [1] L. Howard, *The Climate of London* (1818), International Association for the Urban Climate, Incropera, Incropera's Principles of Heat and Mass Transfer, Global Edition, eighth ed., Wiley, 2017.
- [2] T.R. Oke, The distinction between canopy and boundary-layer urban heat islands, *Atmosphere* 14 (4) (1976) 268–277, <https://doi.org/10.1080/00046973.1976.9648422>.
- [3] M. Georgescu, Urban Adaptation Can Roll Back Warming of Emerging Megapolitan Regions, 2014. PNAS, www.pnas.org/cgi/doi/10.1073/pnas.1322280111.
- [4] WHO, COP24 Special report, Health & Climate Change, 2018. <https://apps.who.int/iris/bitstream/handle/10665/276405/9789241514972-eng.pdf?ua=1>.
- [5] W. Peng, X. Yuan, W. Gao, R. Wang, W. Chen, Assessment of urban cooling effect based on downscaled land surface temperature: a case study for Fukuoka, Japan, *Urban Climate* 36 (2021) 100790, <https://doi.org/10.1016/j.uclim.2021.100790>.
- [6] J. Cao, W. Zhou, Z. Zheng, T. Ren, W. Wang, Within-city spatial and temporal heterogeneity of air temperature and its relationship with land surface temperature, *Landsc. Urban Plann.* 206 (2021) 103979, <https://doi.org/10.1016/j.landurbplan.2020.103979>.
- [7] M. Santamouris, *Cooling the cities – a review of reflective and green roof mitigation technologies to fight heat island and improve comfort in urban environments*. Group Building Environmental Research, Physics Department, University of Athens, Athens, Greece, 2012.
- [8] H. Andoni, S. Wonorahardjo, A review on mitigation technologies for controlling urban heat island effect in housing and settlement areas, *IOP Conf. Ser. Earth Environ. Sci.* 152 (2017), 012027, <https://doi.org/10.1088/1755-1315/152/1/012027>.
- [9] B.G. Heusinkveld, G.J. Steeneveld, L.W.A. van Hove, C.M.J. Jacobs, A.A. M. Holtslag, An urban climate assessment and management tool for combined heat and air quality judgements at neighbourhood scales, *Resour. Conserv. Recycl.* 132 (2014) 204–217, <https://doi.org/10.1016/j.resconrec.2016.12.002>.
- [10] L.W.A. van Hove, C.M.J. Jacobs, B.G. Heusinkveld, J.A. Elbers, B.L. van Driel, Temporal and spatial variability of urban heat island and thermal comfort within the Rotterdam agglomeration, *Build. Environ.* 83 (2015) 91–103, <https://doi.org/10.1016/j.buildenv.2014.08.029>.
- [11] M. Masoudi, P.Y. Tan, Multi-year comparison of the effects of spatial pattern of urban green spaces on urban land surface temperature, *Landsc. Urban Plann.* 184 (2019) 44–58, <https://doi.org/10.1016/j.landurbplan.2018.10.023>.
- [12] M. Nuruzzaman, Urban heat island: causes, effects and mitigation measures - a review, *Int. J. Environ. Monit. Anal.* 3 (2) (2015) 67–73, <https://doi.org/10.11648/j.ijema.20150302.15>.
- [13] A. Aflaki, M. Mirnezhad, A. Ghaffarianhoseini, A. Ghaffarianhoseini, H. Omrany, Zhi-HuaWang, H. Akbari, Urban heat island mitigation strategies: a state-of-the-art review on Kuala Lumpur, Singapore and Hong Kong Cities 62 (2016) 131–145, <https://doi.org/10.1016/j.cities.2016.09.003>.
- [14] L.S. Chalmin-Pui, J. Roe, A. Griffiths, N. Smyth, T. Heaton, A. Clayden, R. Cameron, "It made me feel brighter in myself" - the health and well-being impacts of a residential front garden horticultural intervention, *Landsc. Urban Plann.* 206 (2021) 103979, <https://doi.org/10.1016/j.landurbplan.2020.103979>.
- [15] C.N. Hewitt, K. Ashworth, A.R. MacKenzie, Using green infrastructure to improve urban air quality (GI4AQ), *Ambio* 49 (2020) 62–73, <https://doi.org/10.1007/s13280-019-01164-3>.
- [16] G.J. Steeneveld, J.O. Klomp maker, R.J.A. Groen, A.A.M. Holtslag, An urban climate assessment and management tool for combined heat and air quality judgements at neighbourhood scales, *Resour. Conserv. Recycl.* 132 (2018) 204–217, <https://doi.org/10.1016/j.resconrec.2016.12.002>.
- [17] M. Ottel , *The Green Building Envelope, Vertical Greening PhD Thesis*, Delft University of Technology, 2013.
- [18] A. Speak, L. Montagnani, C. Wellstein, S. Zerbe, The influence of tree traits on urban ground surface shade cooling, *Landsc. Urban Plann.* 197 (2020) 103748, <https://doi.org/10.1016/j.landurbplan.2020.103748>.

- [19] S. Wonorahardjo, I.M. Sutjahja, Y. Mardiyati, H. Andoni, D. Thomas, R.A. Achsan, S. Steven, Characterising thermal behaviour of buildings and its effect on urban heat island in tropical areas, *International Journal of Energy and Environmental Engineering* 11 (2020) 129–142, <https://doi.org/10.1007/s40095-019-00317-0>.
- [20] M.-T. Hoelscher, T. Nehls, B. Jänick, G. Wessolek, Quantifying Cooling Effects of Facade Greening: Shading, Transpiration and Insulation, *Energy and Buildings*, 2015, <https://doi.org/10.1016/j.enbuild.2015.06.047>.
- [21] T.R. Oke, *The urban energy balance*. Progress in Physical Geography, 1988. <https://journals.sagepub.com/doi/10.1177/030913338801200401>.
- [22] Y.J. Kwon, D.K. Lee, Thermal comfort and longwave radiation over time in urban residential complexes, *Sustainability* 11 (2019) 2251, <https://doi.org/10.3390/su11082251>.
- [23] M. Ottelé, K. Perini, Comparative experimental approach to investigate the thermal behaviour of vertical greened façades of buildings, *Ecol. Eng.* 108 (2018), <https://doi.org/10.1016/j.ecoleng.2017.08.016>. Prt A, 152–161.
- [24] M. Carpio, Á. González, M. González, K. Verichev, Influence of pavements on the urban heat island phenomenon: a scientific evolution analysis, *Energy Build.* 226 (2020) 110379.
- [25] X. Sun, C.B. Zou, B. Wilcox, E. Stebler, Effect of vegetation on the energy balance and evapotranspiration in tallgrass prairie: a paired study using the eddy-covariance method, *Boundary-Layer Meteorol.* 170 (2019) 127–160, <https://doi.org/10.1007/s10546-018-0388-9>.
- [26] J.M. Schouten, Een Boompje opzetten, *Houtblad Het*, jaargang 32 nummer 6, <https://www.houtwereld.nl/author/jan-maurits-schouten/>, 2020.
- [27] T. Denters, *The Flora of the Urban District, Gorteria*, 1998.
- [28] A. Ossola, G.D. Jenerette, A. McGrath, W. Chow, L. Hughes, M.R. Leishman, Small vegetated patches greatly reduce urban surface temperature during a summer heatwave in Adelaide, Australia, *Landsc. Urban Plann.* 209 (2021) 104046, <https://doi.org/10.1016/j.landurbplan.2021.104046>.
- [29] K.B. Byrne, G. Kiely, Leahy p, CO₂ fluxes in adjacent new and permanent temperate grasslands, *Agric. For. Meteorol.* 135 (2005) 82–92, <https://doi.org/10.1016/j.agrformet.2005.10.005>.
- [30] Knmi Data, source: <https://projects.knmi.nl/klimatologie/uurgegevens/selectie.cgi>, 2020.
- [31] M. Santamouris, *Environmental Design of Urban Buildings, an Integrated Approach*, Earthscan London, 2006.
- [32] C. Richard, G. Doré, C. Lemieux, J.-P. Bilodeau, J. Haure-Touzé, Albedo of pavement surfacing materials: in situ measurements, *Cold Regions Engineering* (2015).
- [33] L. Romeijn, *Monitoring Albedo of Urban Surfaces under Wet and Dry Conditions*, repository TU Delft CiTG, 2014 pag. 8.
- [34] B. Xiao, M.A. Bowker, Moss-biocrusts strongly decrease soil surface albedo, altering land-surface energy balance in a dryland ecosystem, *Sci. Total Environ.* 741 (2020) 140425, <https://doi.org/10.1016/j.scitotenv.2020.140425>.
- [35] A. Ångström, *The Albedo of Various Surfaces of Ground*, Taylor & Francis, Ltd. on behalf of Swedish Society for Anthropology and Geography, 1925, <https://doi.org/10.2307/519495>.
- [36] U. Niinemets, M. Tobias, Canopy leaf area index at its higher end: dissection of structural controls from leaf to canopy scales in bryophytes, *New Phytol.* 223 (2019) 118–133, <https://doi.org/10.1111/nph.15767>.
- [37] B. Bond-Lamberty, S. Gower, DOI, Estimation of Stand-Level Leaf Area for Boreal Bryophytes *Oecologia*, May 2007, <https://doi.org/10.1007/s00442-006-0619-5> (Source: PubMed).
- [38] Y. He, X. Xulin Guo, J.F. Wilmshurst, Comparison of different methods for measuring leaf area index in a mixed grassland, *Can. J. Plant Sci.* 87 (2007) 803–813.
- [39] L.G. Pérez, J. Coma, S. Sol, F.L. Cabeza, Green facade for energy savings in buildings: the influence of leaf area index and facade orientation on the shadow effect, *Appl. Energy* 187 (2017) 424–437, <https://doi.org/10.1016/j.apenergy.2016.11.055>.
- [40] S. Wolter, J. Diebel, F.-G. Schroeder, Development of hydroponic systems for urban facade greenery. *ISHS Acta Horticulturae 843: International Symposium on Soilless Culture and Hydroponics*, 2009.
- [41] O. Starry, *The Comparative Effects of Three Sedum Species on Green Roof Stormwater Retention*, in: in Partial Fulfilment of the Requirements for the Degree of Doctor of Philosophy, Dissertation submitted to the Faculty of the Graduate School of the University of Maryland, College Park, 2013, p. 71.
- [42] M. Kluge, Is *Sedum acre* L. a CAM plant? *Oecologia* 29 (1977) 77–83, <https://doi.org/10.1007/BF00345364>.
- [43] K. Winter, J.A.M. Holtum, Facultative crassulacean acid metabolism (CAM) plants: powerful tools for unravelling the functional elements of CAM photosynthesis, *J. Exp. Bot.* 65 (Issue 13) (July 2014) 3425–3441, <https://doi.org/10.1093/jxb/eru063>.